

THE SIMULATION OF THE MOTION OF SOLID PARTICLES IN THE TURBULENT FLOW OF INDUCTION CRUCIBLE FURNACES

Mihails Ščepanskis^{*}, Andris Jakovičs[†] and Bernard Nacke^{††}

^{*†}Laboratory for Mathematical Modelling of Environmental and Technical Processes,
University of Latvia
Zellu str. 8, LV-1002, Riga (Latvia)
e-mail: {mihails.scepanskis,andris.jakovics}@lu.lv

^{††}Institute of Electrotechnology, Leibniz University of Hanover
Wilhelm-Busch str. 4, 30167, Hanover (Germany)
nacke@etp.uni-hannover.de

Key words: LES, particles, OpenFOAM, ICF

Abstract. *The process of the motion of solid particles in the metal melt is simulated in the present paper. The model consists of the flow and the particles movement calculation at each time step. The simulation of the EM induction governed turbulent flow is carried out using the Large Eddy Simulation (LES) method with the Smagorinsky subgrid viscosity model. The motion of the solid non-conductive particles is simulated using the Lagrangian equation that takes into account drag, buoyancy, EM, lift, acceleration and added mass forces. The application of two models of the particle collisions with the wall (non-slipping by the wall and slipping by the wall) is analyzed for particles with different densities. The particles with different densities are considered. The typically scheme of the motion of the particle cloud is obtained and the regions of the concentration of big particles are estimated.*

1 INTRODUCTION

The problem of solid particle tracking in metal melts is associated with different industrial processes. The alloying particles (such as Mo, Ni, Si etc.) are mixed into the steel melt to increase some properties, such as strength, hardness, wear resistance and others. In this case the goal is to reach the homogeneous distribution of the particles in the short time. The other problem is associated with the impurities that come to the melt from the dirty melting material (such as SiO_2 , MgO etc.) and from the erosion of the furnace wall (such as Al_2O_3). These particles can deposit on the wall of the furnace and change the configuration of the flow and the electromagnetic (EM) field.

The densities of particles are different, they can be lighter and heavier than the melt density. The density of some admixture materials and metals is shown on Table 1. The light particles can form the “slag” on the top surface [1].

chemical element or formula	density, g/cm^3	origin
Mo	10.28	alloying particles
Ni	8.908	
Si	2.3290	
Al_2O_3	3.97	wall erosion
MgO	3.65	impurities
SiO_2	2.32	

Table 1: The possible admixtures in the melt and their origin.

The problem of particle tracking is considered in this paper. On the basis of the particle transport model the process of the homogenization of the alloying particles is analyzed. The possible areas of the particle deposition and their properties for cylindrical ICF are also estimated.

The stationary motion of solid particles in the averaged flow in ICF [2] and non-stationary (turbulent) motion under the influence of drag, buoyancy and EM forces in unsteady flow in ICF by using LES method [3] was analyzed. Physically more sophisticated model that additionally includes lift, acceleration and added mass forces is presented in this paper. The influence of these forces on the motion of the particles is analyzed.

The different models of the behaviour of the particle close to the wall are considered. One model is not taking into account the size of the particles and considers collision when the center of the particle reaches the wall. The another one takes into account the size of the particle and moves it to the distance of the radius from the wall if it is closer. The results of simulation using these two models are significantly different for some cases; the present paper considers the analysis of these cases.

The simulation is carried out for the model of the cylindrical ICF which is typical object for the inductive melting processes. The sketch of ICF is shown on Figure 1 and the sizes and other parameters are shown on Table 2. The laboratory ICF with such parameters was used in some previous theoretical and experimental investigations (for example in [4,5]), therefore we also use this ICF to have the possibility to compare the results. For the same reason the flow of the Wood’s metal is considered.

property	value
inductor frequency	365 Hz
inductor current	2000 A
melt and inductor height	570 mm
crucible radius	158 mm
number of inductor turns	12

Table 2: The properties of laboratory scale ICF.

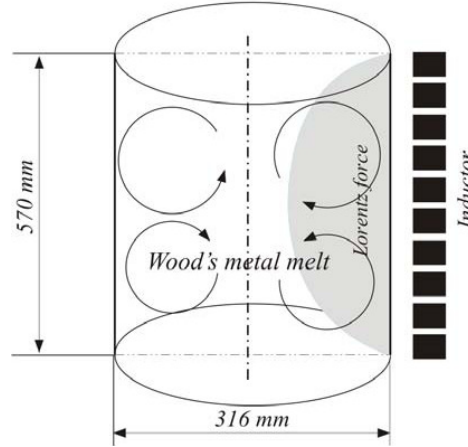


Figure 1: The design of ICF with the sketch of the typical vortices of the mean flow.

2 THEORETICAL ANALYSIS AND MODEL

The numerical simulation is carried out using free code OpenFOAM software.

Present model includes the flow and the particle motion simulation. The turbulent flow simulation is carried out using the LES method with the Smagorinsky subgrid viscosity model [4]. The flow is governed by electromagnetic force and thermal buoyancy force in the Boussinesq approximation [4]. The adiabatic and the convective thermal boundary conditions are considered.

The result of the flow simulation is the field of the flow velocities at each time step that is used for the particle trajectories calculation. The Lagrangian equation describes the motion of the particles.

2.1 The theoretical investigation of the particle motion

Let us initially consider a movable spherical particle in a still liquid. This case is same as the case when the liquid moves and the particle is immovable. The non-stationary Navier-Stokes equation that describes the motion of the liquid:

$$\frac{\partial \mathbf{u}_f}{\partial t} = -\frac{1}{\rho} \cdot \nabla p + \nu \cdot \Delta \mathbf{u}_f, \quad (1)$$

where \mathbf{u}_f is velocity of the flow (the origin of the flow motion is only the motion of the particle), p is pressure, ρ is density, ν is kinematic viscosity.

Using *curl* operator we can get rid of the pressure in Eq. 1 [6] and write this equation for a flow function ψ in a spherical coordinate system [7,8]:

$$\left(L - \frac{1}{\nu} \frac{\partial}{\partial t} \right) L \psi = 0, \quad (2)$$

where $L = \frac{\partial^2}{\partial r^2} + \frac{\sin \theta}{r^2} \frac{\partial}{\partial \theta} \left(\frac{1}{\sin \theta} \frac{\partial}{\partial \theta} \right)$ is differential operator. The boundary conditions are

$$\frac{1}{a^2 \sin \theta} \frac{\partial \psi}{\partial \theta} = u_p(t) \cdot \cos \theta ; \quad \frac{1}{a \sin \theta} \frac{\partial \psi}{\partial r} = u_p(t) \cdot \sin \theta ,$$

where $u_p(t)$ is velocity of the particle, a is the radius of the particle.

The solution of Eq. 2 is found in such form [7]:

$$\psi(r, \theta, t) = \sin^2 \theta \cdot f(r, t) + \cos \theta \cdot \sin^2 \theta \cdot g(r, t) ,$$

where

$$\begin{aligned} \left(L - \frac{1}{\nu} \frac{\partial}{\partial t} \right) L \psi &= 0, \quad L_1 \equiv \frac{\partial^2}{\partial r^2} - \frac{2}{r^2}; \\ \left(L_2 - \frac{1}{\nu} \frac{\partial}{\partial t} \right) L_2 \psi &= 0, \quad L_2 \equiv \frac{\partial^2}{\partial r^2} - \frac{6}{r^2}. \end{aligned} \quad (3)$$

The form of the expression for the force \mathbf{F} on the spherical particle obtained by evaluating the stress on the surface and integrating is as follows [7]:

$$\frac{\mathbf{F}}{\rho \cdot V_p} = \frac{du_p}{dt} + \left\{ \frac{1}{r} \frac{\partial^2 f}{\partial r \partial t} + \frac{\nu}{r} \cdot \left(\frac{2}{r^2} \frac{\partial f}{\partial r} + \frac{2}{r} \frac{\partial^2 f}{\partial r^2} - \frac{\partial^3 f}{\partial r^3} \right) \right\} \Bigg|_{r=a} ,$$

where V_p is volume of the particle. It transpires that this is independent of g . Hence only the solution to Eq. 3 for $f(r, t)$ need be sought to find the force on a spherical particle.

Eq. 3 is solved using the Laplace transformation [9] for non-slip boundary conditions [7,8], and force \mathbf{F} is as follows [7]:

$$\frac{\mathbf{F}}{\rho \cdot V_p} = -\frac{1}{2} \frac{d\mathbf{u}_p}{dt} + \frac{3}{2} \frac{d\mathbf{u}_f}{dt} + \frac{9\nu}{2a^2} \cdot (\mathbf{u}_f - \mathbf{u}_p) + \frac{9}{2a} \sqrt{\frac{\nu}{\pi}} \cdot \int_0^t \frac{d(\mathbf{u}_f - \mathbf{u}_p)}{d\tau} \frac{d\tau}{\sqrt{t-\tau}} . \quad (4)$$

We can compare Eq. 4 with result obtained for potential liquid and generalize it by replacing $\frac{d\mathbf{u}_f}{dt}$ to $\frac{D\mathbf{u}_f}{Dt}$, where $\frac{D}{Dt}$ is material derivation [7,10].

The summand that contains the integral in Eq. 4 is too complex for numerical modeling while its contribution to the force is not so big because of the oscillation of the flow acceleration [4].

It is necessary to note that the flow in our case is not the Stokes flow. The Reynolds number for the particles $\text{Re}_p = aU/\nu$ was estimated [4] ($U = u_f - u_p$). Acceleration parameter $Ac = U^2/a\dot{U}$ (\dot{U} is relative acceleration) was also estimated. Taking into account these estimations we should change the coefficients in some summands in Eq. 4. The Schiller-Naumann approximation for the drag coefficient C_D [11] and the Odar-Hamilton approximation for acceleration coefficient C_A [12] are used:

$$C_D = \frac{1}{\tau_p} \left(1 + 0.15 \cdot \text{Re}_p^{0.687} \right), \quad (5)$$

$$C_A = 2.1 - \frac{0.132}{0.12 + Ac^2},$$

where $\tau_p = a^2 S / 18\nu$ is Stokes relaxation time, S is ratio of particle density to liquid density: $S = \rho_p / \rho_f$.

The density of the liquid ρ_f and the density of the particles ρ_p are different, so we should take into account buoyancy force. There is EM field that influence the motion of the particle, so we also should take into account EM force. Lift force appears due to the flow circulation and is significant in some regions of the crucible. The Legendre-Magnaudet approximation for the lift coefficient C_L [13] is used:

$$C_L(\text{Re}_p) = \frac{1}{2} \frac{1 + 16 \cdot \text{Re}_p^{-1}}{1 + 29 \cdot \text{Re}_p^{-1}}.$$

Thus the Lagrangian equation for non-conductive particle motion is so:

$$\left(1 + \frac{C_A \rho_f}{2 \rho_p}\right) \cdot \frac{d\mathbf{u}_p}{dt} = C_D \cdot \mathbf{U} + \left(1 - \frac{\rho_f}{\rho_p}\right) \cdot \mathbf{g} - \frac{3}{4} \frac{1}{\rho_p} \mathbf{f}_{\text{em}} + \frac{\rho_f}{\rho_p} C_L \boldsymbol{\xi} + \left(1 + \frac{C_A}{2}\right) \cdot \frac{D\mathbf{u}_f}{Dt}, \quad (6)$$

where coefficients C_D , C_L and C_A depends on Re_p ; vector $\mathbf{f}_{\text{em}} = [\mathbf{j} \times \mathbf{B}]$ is the Lorentz force density, \mathbf{j} is a current density, \mathbf{B} is magnetic field induction; vector $\boldsymbol{\xi} = [\mathbf{U} \times [\nabla \times \mathbf{U}]]$ describes the lift force.

The structure of Eq. 6 is following:

$$\left[\frac{d\mathbf{u}_p}{dt} + \text{added mass 1}\right] = [\text{drag}] + [\text{buoyancy}] + [EM] + [\text{lift}] + [\text{acceleration} + \text{added mass 2}]$$

The added mass force is divided in two parts (*added mass 1* and *added mass 2*) like it is implemented in the algorithm.

Particle velocity \mathbf{u}_p is not a vector field, but a single vector for each particle, thus suppose $\text{curl} \mathbf{u}_p = \mathbf{0}$ and get for $\boldsymbol{\xi}$

$$\boldsymbol{\xi} = [\mathbf{U} \times [\nabla \times \mathbf{U}]] = [\mathbf{u}_f \times [\nabla \times \mathbf{u}_f]] - [\mathbf{u}_p \times [\nabla \times \mathbf{u}_f]] \equiv \boldsymbol{\eta} - [\mathbf{u}_p \times \boldsymbol{\mu}].$$

Vector $\boldsymbol{\eta}$ approximately describes the magnitude of lift force.

2.2 The algorithm of the simulation

The scheme of the algorithm is shown on Figure 2. The first step of numerical algorithm is the fluid velocity field calculation using LES method; the second one is the particles motion simulation. Both steps are implemented at each time step.

We consider particle transport model with several assumptions made:

- the particle-particle interaction is negligible,
- all particles are rigid spheres,
- the particles do not affect the structure and the velocities of the flow,
- the particles can slide along the wall but cannot stick to the wall (the processes of the surface diffusion and the deformation of the particle are not considered).

Eq. 5 is solved numerically using the implicit difference scheme. Thus we get the system of linear algebraic equation for vector \mathbf{u}_p components. This system is solved using Gauss method.

Two models of the behaviour of the particles close to the wall are considered. *Model 1* neglect the size of the particles in the case of collisions with the wall, i. e. the collision takes place when the center of the particle reaches the wall. It will be shown in Chapter 3.2 that *Model 1* simulates the case when the particle can not slip by the wall. The rough wall can make such conditions. *Model 2* takes into account the size of the particle and moves the particle to the distance of the radius from the wall if it is close. In this case the particle can slip by the wall. Both models simulate the collision type when some energy dissipates:

$$u_p^{n'} = \varepsilon \cdot u_p^n,$$

$$u_p^{t'} = (1 - \mu) \cdot u_p^t,$$

where u_p^n and u_p^t are normal and tangential components of the particle velocity before collision; $u_p^{n'}$ and $u_p^{t'}$ are normal and tangential components of the particle velocity after collision; ε and μ are the coefficients of restitution and friction respectively. In the present simulation $\varepsilon = 0.8$ and $\mu = 0.2$.

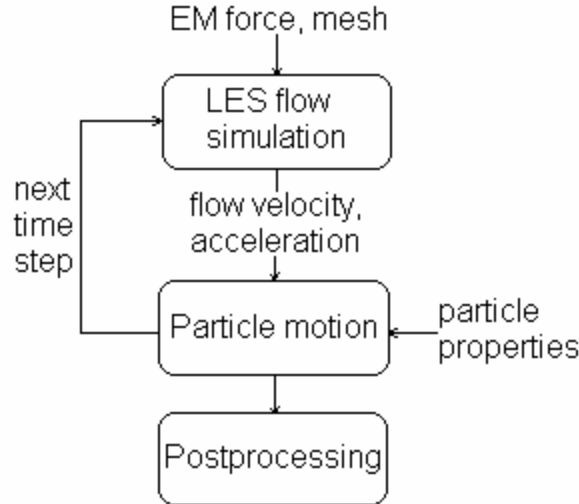


Figure 2: The scheme of the algorithm.

3 RESULTS OF SIMULATION

The particles are input in the developed turbulent flow in a plane near the top surface of the crucible (1.5 cm deep). This particle initial distribution qualitatively corresponds to the industrial case of the admixture components inputting in a melt.

The time step 0.005 s is used in calculations; the mesh has about 3 million elements; the typical time of the calculation of 10 s on 1 processor is about 3 days.

3.1 The analysis of the influence of the different forces on the particle trajectory

The number of numerical experiments was carried out taking into account different forces. Using the results of the experiments the influence of these forces on particle motion in the turbulent EM induced flow was analyzed.

Drag force is basic reason of the particle motion. The particle is accelerated when the flow velocity is more than the particle one and is decelerated in the opposite case. The less the size of the particle, the bigger is drag force, thus the motion of the small

particles repeats the flow motion. The greater particles have more inertia and react to the changes of the flow velocity more slowly. The dependence of drag force on the particle size is not linear (Eq. 5). This is the only force that divided to the mass significantly depends on the size of the particle.

EM force is significant in the skin layer near the side wall of the crucible:

$$\delta = \sqrt{\frac{2}{\mu_0 \sigma \omega}},$$

where μ_0 is permeability of free space (magnetic field constant); σ is electrical conductivity; ω is cyclic frequency. In considered case $\delta = 2.6 \text{ cm}$.

Then the non-conductive particle comes to this layer the EM force try to move it in the direction of the wall. On the Figure 3 we can compare the trajectories of the particle, when for the one EM force is taken into account and for the other is not taken; so we can see that due to EM force the trajectories separate near the wall, particles come to different flow conditions and their further trajectories are totally different.

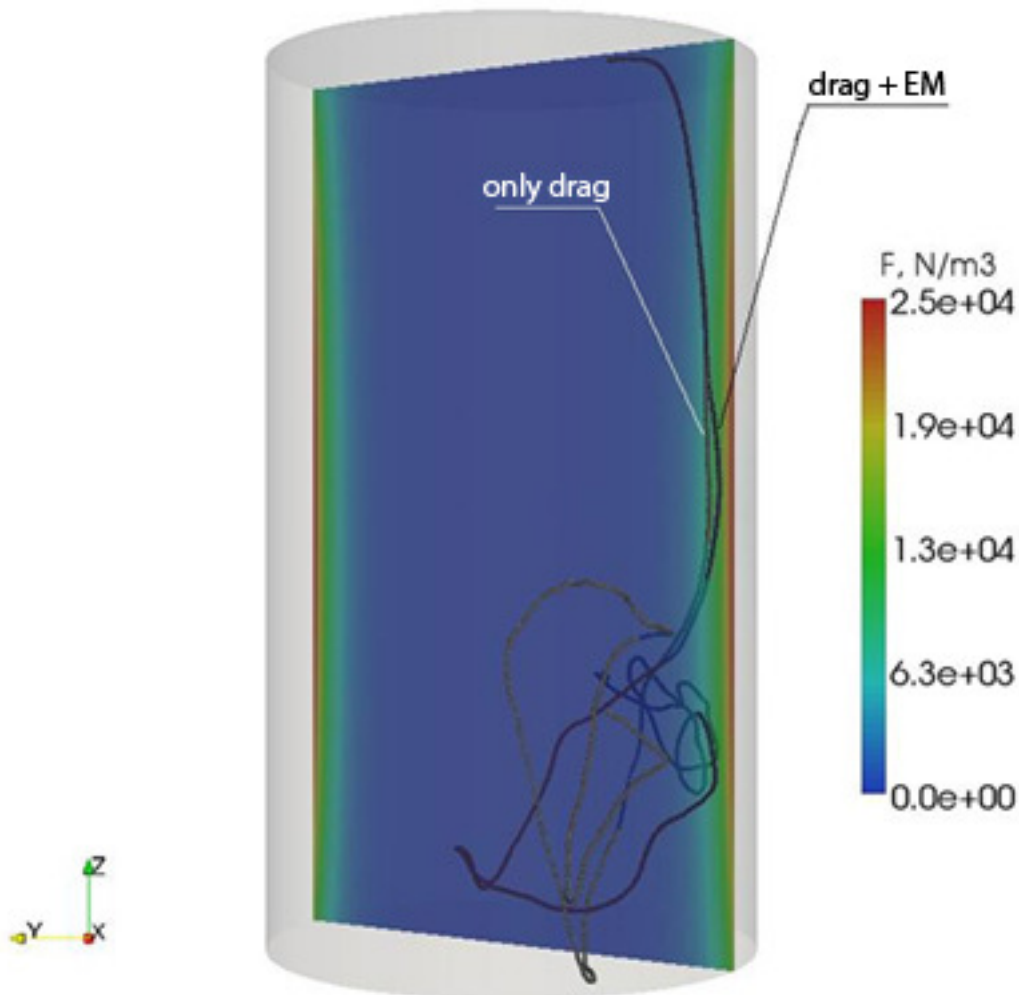


Figure 3: Stationary EM force density field in vertical plane and the trajectories of the particles taking into account EM force and not.

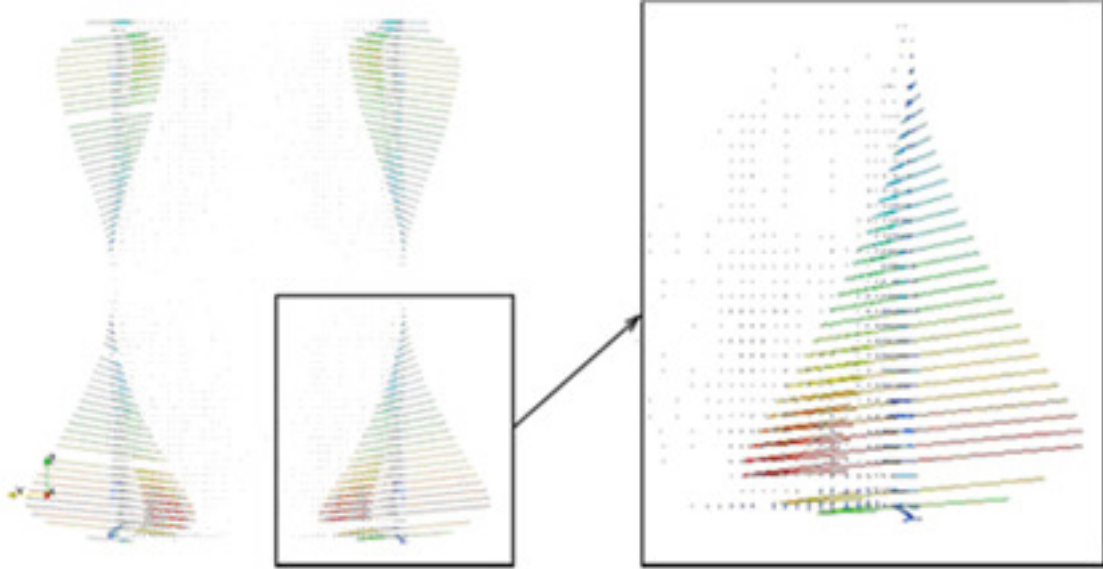


Figure 4: Distribution of vector component $\boldsymbol{\eta} \equiv [\mathbf{u}_f \times [\nabla \times \mathbf{u}_f]]$ of lift force for stationary EM induced flow with two typical flow eddies (Figure 5 (a)). The angular component of lift force in the stationary flow is zero.

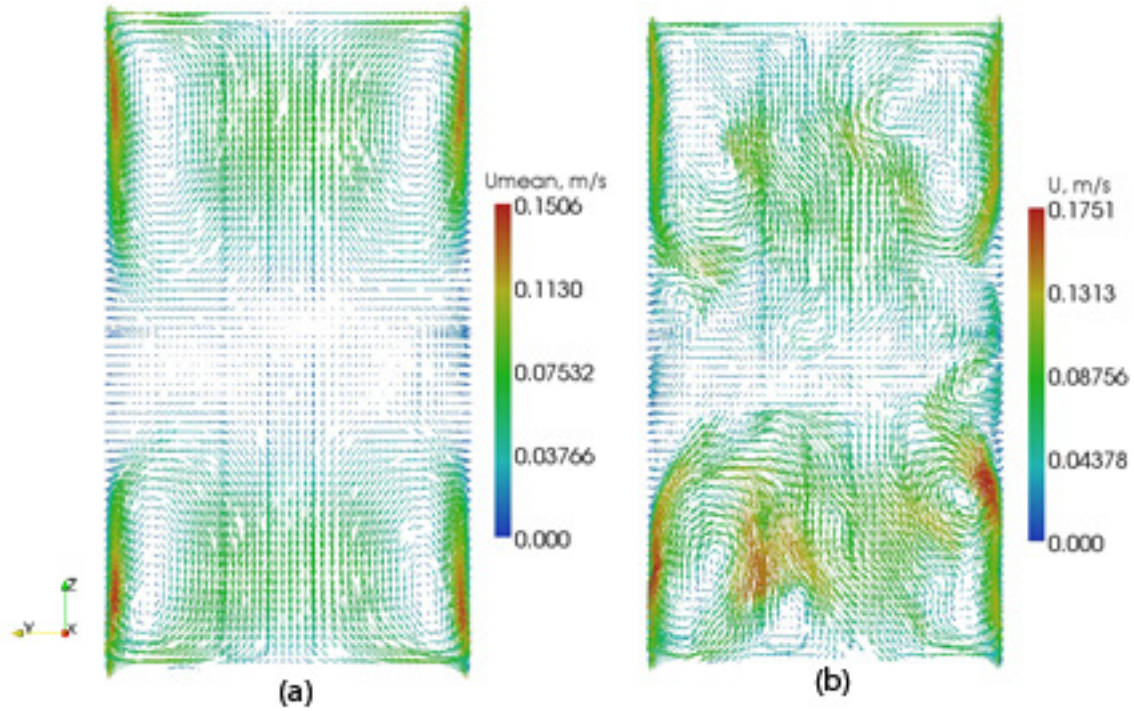


Figure 5: (a) – average flow velocity in ICF; (b) – momentary flow velocity at 45 s.

Lift force is significant in the areas where both velocity magnitude and derivative of velocity magnitude are significant. Such stationary areas are situated near the wall of the crucible in the zones of the eddies (Figure 4). In a thin layer near the wall the velocity reaches maximum and the border condition for velocity is $\mathbf{u}_p = 0$. Thus the area derivative of the velocity has different sign in different directions from the point of the velocity maximum r_{\max} (Figure 5 (a)). Lift force tries to move the particle away from the wall if it is very close to the wall ($r > r_{\max}$), and moves it to the wall if it is in the opposite side of the point ($r < r_{\max}$), where the velocity reaches the maximum. Lift force

is significant only in the regions where both rotor of the relative particle velocity $curl \mathbf{U}$ and the relative particle velocity \mathbf{U} are significant. Due to non-stationary turbulent flow simulation some short-term areas, where the lift force is significant, also appears inside of the crucible. When the particle comes to this area, lift force changes its trajectory.

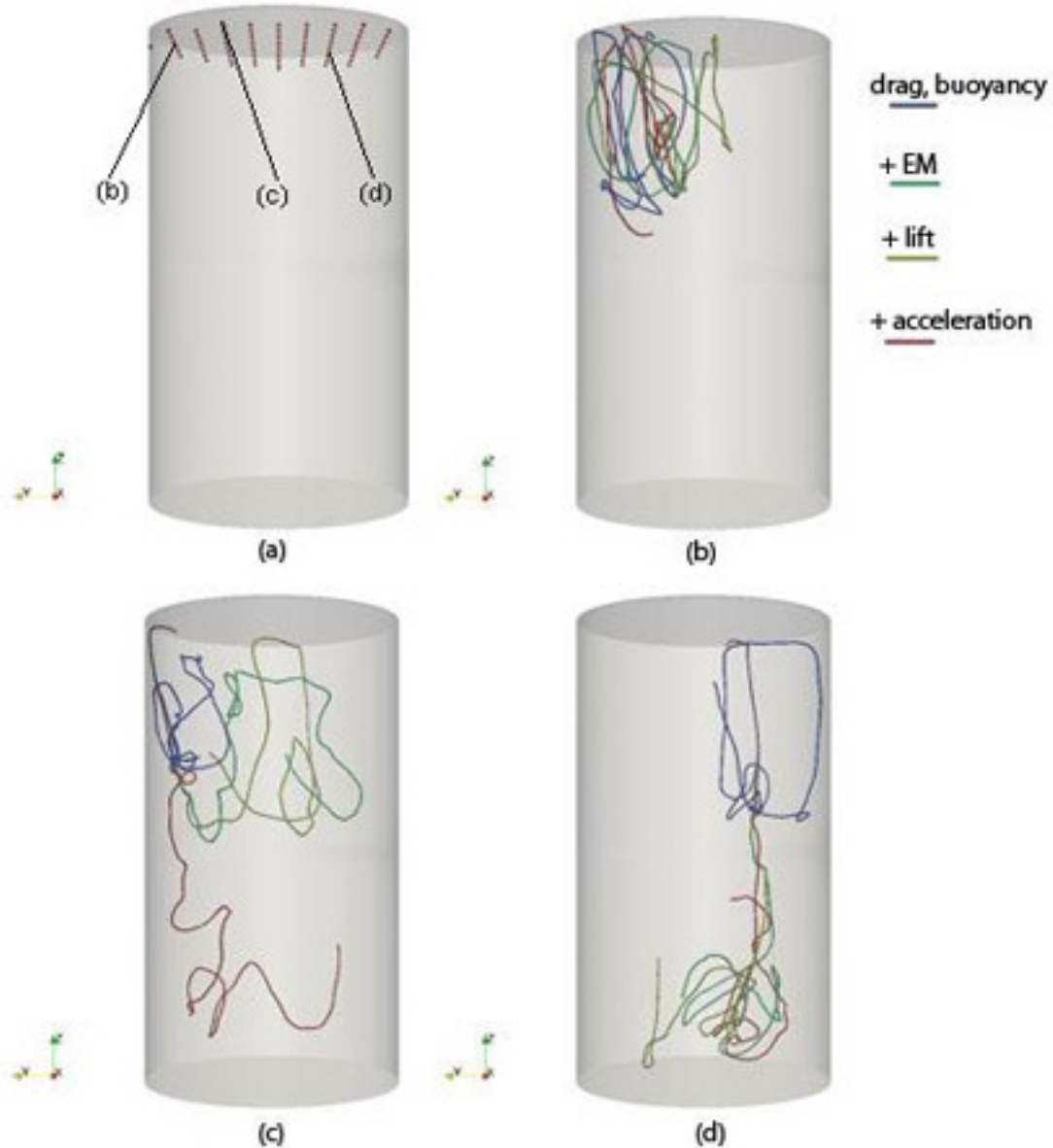


Figure 6: The trajectories of the particles with diameter 0.1 mm. The trajectories are calculated taking into account different forces (are shown in the legend). (a) – the initial position of particles whose trajectories are shown on figures (b) – (d).

Due to non-stationary turbulent flow, areas with significant flow acceleration also transiently appear. Thus acceleration and added mass forces influences the particle motion too.

The examples of trajectories of particles, when some forces are taken into account and not taken, are shown on Figure 6. On Figure 6 (d) we can see that EM force significantly changes the trajectory of the particle and bring it into the lower part of the crucible. There are cases when only acceleration force change the trajectory

significantly, e. g. on Figure 6 (c) acceleration force bring the particle to the lower part of the crucible. Thus it is important to take into account all forces that are considered in the present paper to calculate the trajectory of the solid particle in the EM induced turbulent flow; all mentioned forces are significant and can considerably change the trajectory of the particle. But of course there are some cases when additional forces do not change the trajectory of the particle significantly (Figure 6 (b)).

3.2 The simulation of the particles with different densities

We will use two different models of the behaviour of the particles close to the wall (are described in Chapter 2.2) to simulate the motion of the non-conducting particles with different density in the flow of ICF.

The results that were obtained using the *Model 1* (the size of the particles is not taken into account) and *Model 2* (the particle is moved to the distance of the radius from the wall if it is closer) are shown on Figure 7 and Figure 8 respectively.

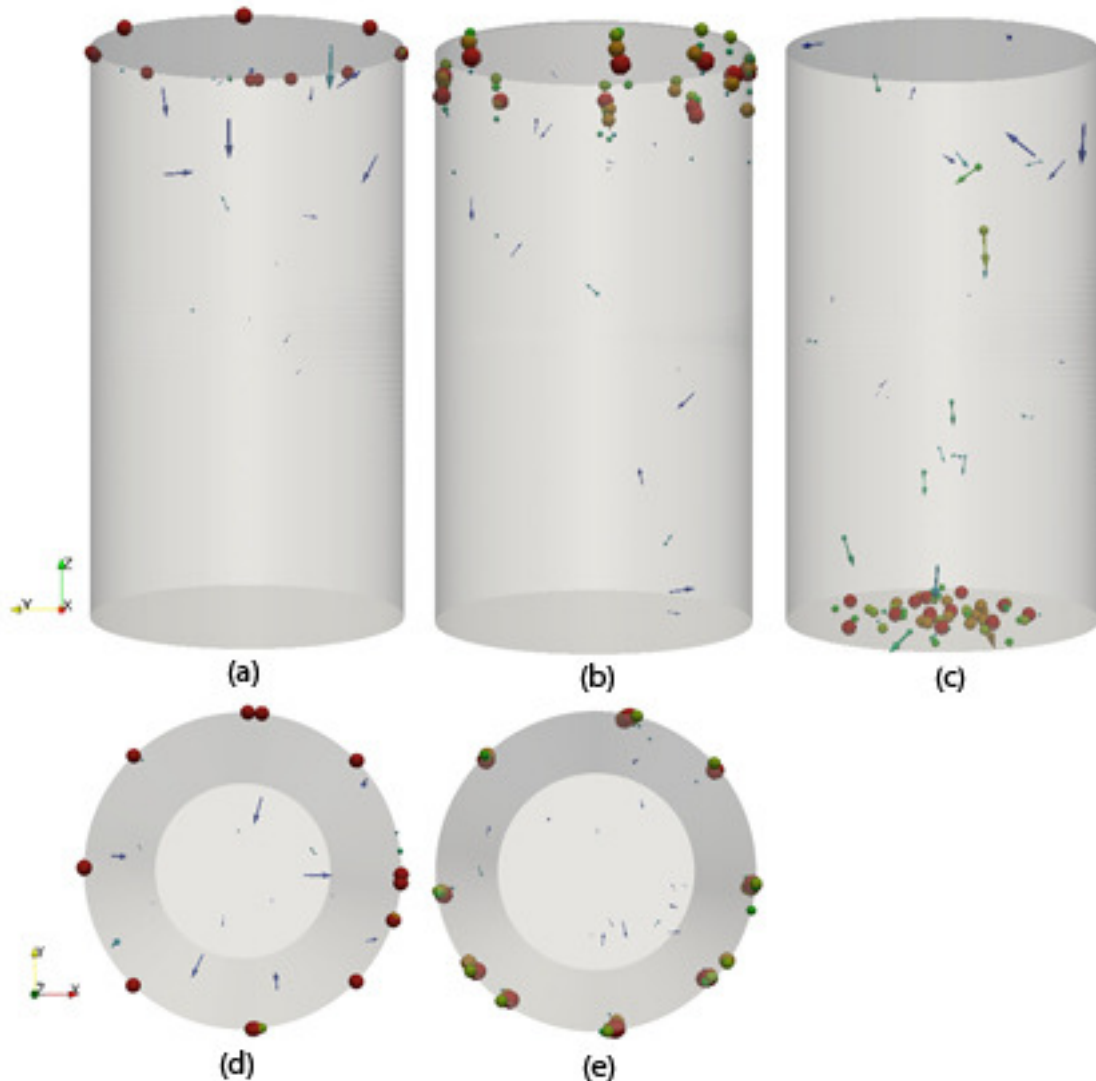


Figure 7: Calculated using *Model 1* (Chapter 2.2). The positions of the particles in ICF after 10 s from the moment when they was input. The diameter of the particles ranges between 0.1 and 1.9 mm. (a), (d) - $\rho_p = \rho_f / 1.5$, (b), (e) - $\rho_p = \rho_f$, (c) - $\rho_p = 1.5 \cdot \rho_f$. The arrows show the direction and the magnitude of the momentary particle velocity at the 10 s. The images are drawn with respect to the optical perspective.

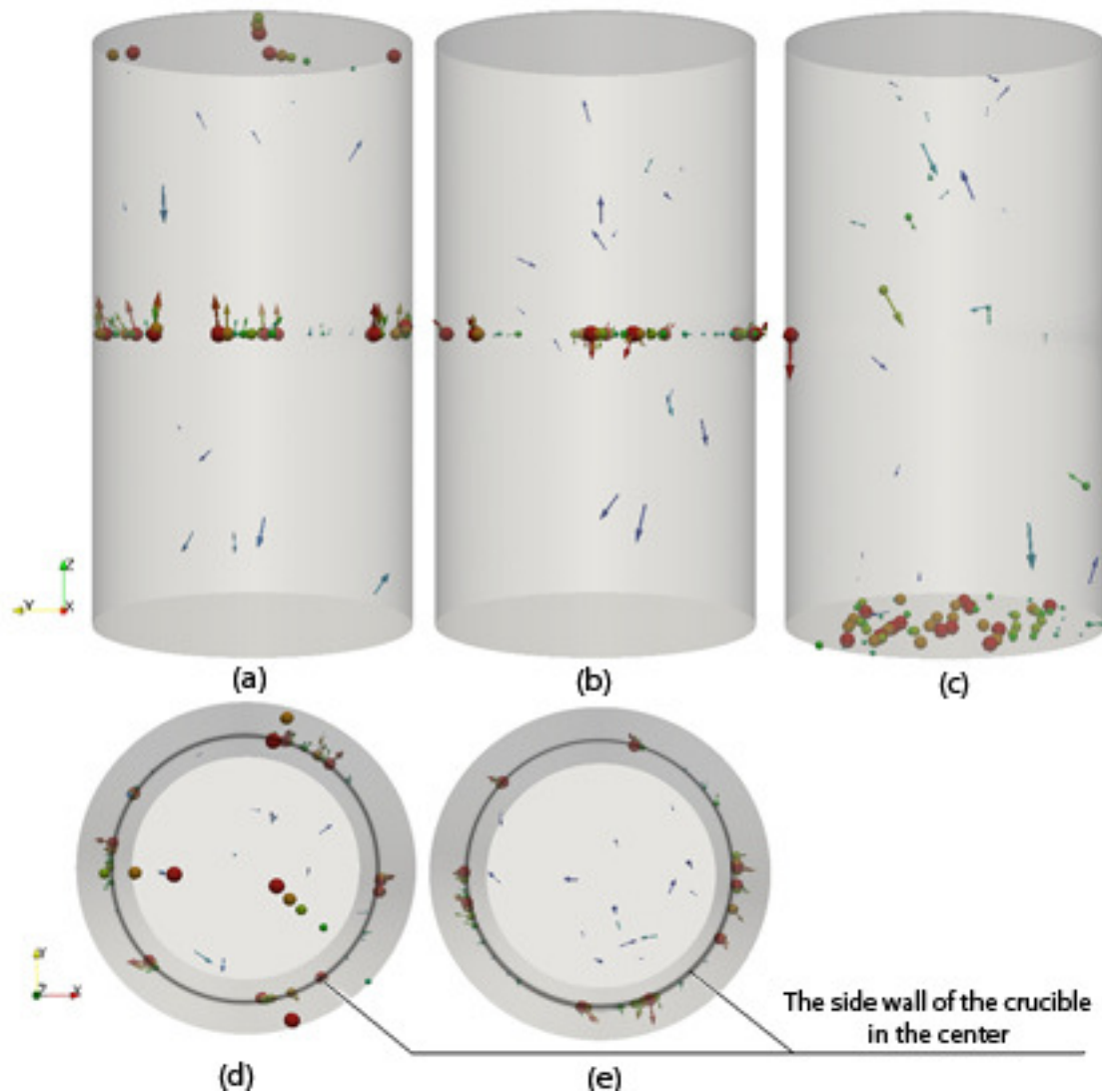


Figure 8: Calculated using *Model 2* (Chapter 2.2). The positions of the particles in ICF after 10 s from the moment than they was input. The diameter of the particles ranges between 0.1 and 1.9 mm. (a), (d) - $\rho_p = \rho_f / 1.5$, (b), (e) - $\rho_p = \rho_f$, (c) - $\rho_p = 1.5 \cdot \rho_f$. The arrows show the direction and the magnitude of the momentary particle velocity at the 10 s. The images are drawn with respect to the optical perspective.

In both models the most heavy particles (Figure 7 (c) and Figure 8 (c)) come to the bottom. Only the small particles move in the flow due to drag force. The results of *Model 1* and *Model 2* are qualitatively similar in this case.

But for the case of the light particles and the case of the particle with density equal to liquid density the results that were obtained using *Model 1* (Figure 7 (a),(b),(d),(e)) and *Mode 2* (Figure 8 (a),(b),(d),(e)) are significantly different.

Using *Model 1* we obtain the result that big particles with the density equal to the liquid density are concentrated on the wall near the top surface of the crucible (Figure 7 (b),(e)). In this model the size of the particle is not taken into account, thus the particle can com near the wall where, due to non-slip boundary condition, the flow velocity magnitude is negligible, thus the particle stay in this region near the wall. *Model 1* simulates the case when the particle can not slip by the wall. This model can be used in the case of the rough wall.

Model 2 gives us another result: big particles are concentrated near the wall in the middle of the crucible (Figure 8 (b),(e)). The result of *Model 2* in this case is more

physical. The middle zone of the crucible is the zone between two eddies of the averaged flow (Figure 5 (a)). The magnitude of the velocity of the flow in this zone is small (Figure 5 (b)) and EM force is comparatively great in this zone near the wall. Thus big particles are concentrated near the wall in the zone between two eddies. Such a situation is also described in the investigations of the other authors (e. g. [14]).

The same difference between *Model 1* and *Model 2* are in the case of light particles (Figure 7 (a),(d) and Figure 8 (a),(d)). *Model 2* also allow the formation of the “slag” in this case. Such a “slag” is observed in the industrial ICF [1].

Thus *Model 2* should be used to obtain more physical results in the cases of the particles with the density less and approximately equal to the liquid density. We can also conclude that for considered parameters of ICF only the particles with diameter less than 0.3 mm move in the flow. Thus such small particles should be used in the analysis of the evolution of the particle density distribution.

3.3 The evolution of the particle distribution in ICF

The evolution of the particle distribution in ICF is analyzed using *Model 2*. The density of the particle is less than the density of the liquid: $\rho_p = \rho_f/1.5$.

Figure 9 schematically shows the simplified scheme of the motion of the particles cloud. Initially all particles are going down through the zone of the upper eddy near the wall to the middle part (Figure 10 (a)). Then the cloud of the particles separates: one part goes to the zone of the upper eddy and other part to the zone of the lower eddy (Figure 10 (b)). After that the particle exchange between two eddies decreases the difference between the number of the particles in zones of the upper and the lower eddies with the lapse of time.

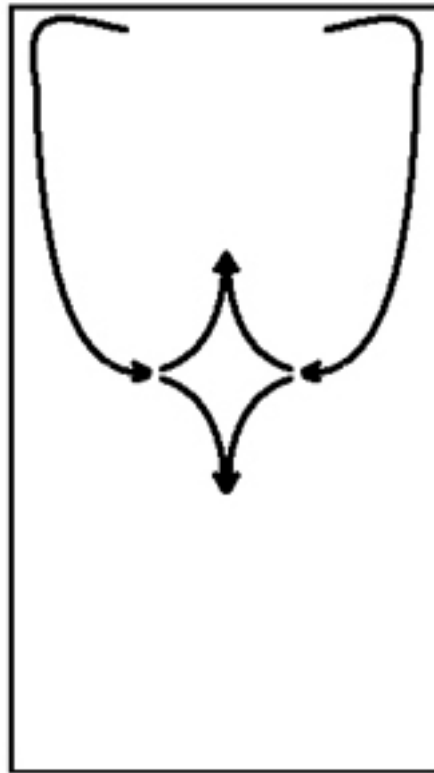


Figure 9: The simplified scheme of the motion of the particle cloud in ICF.

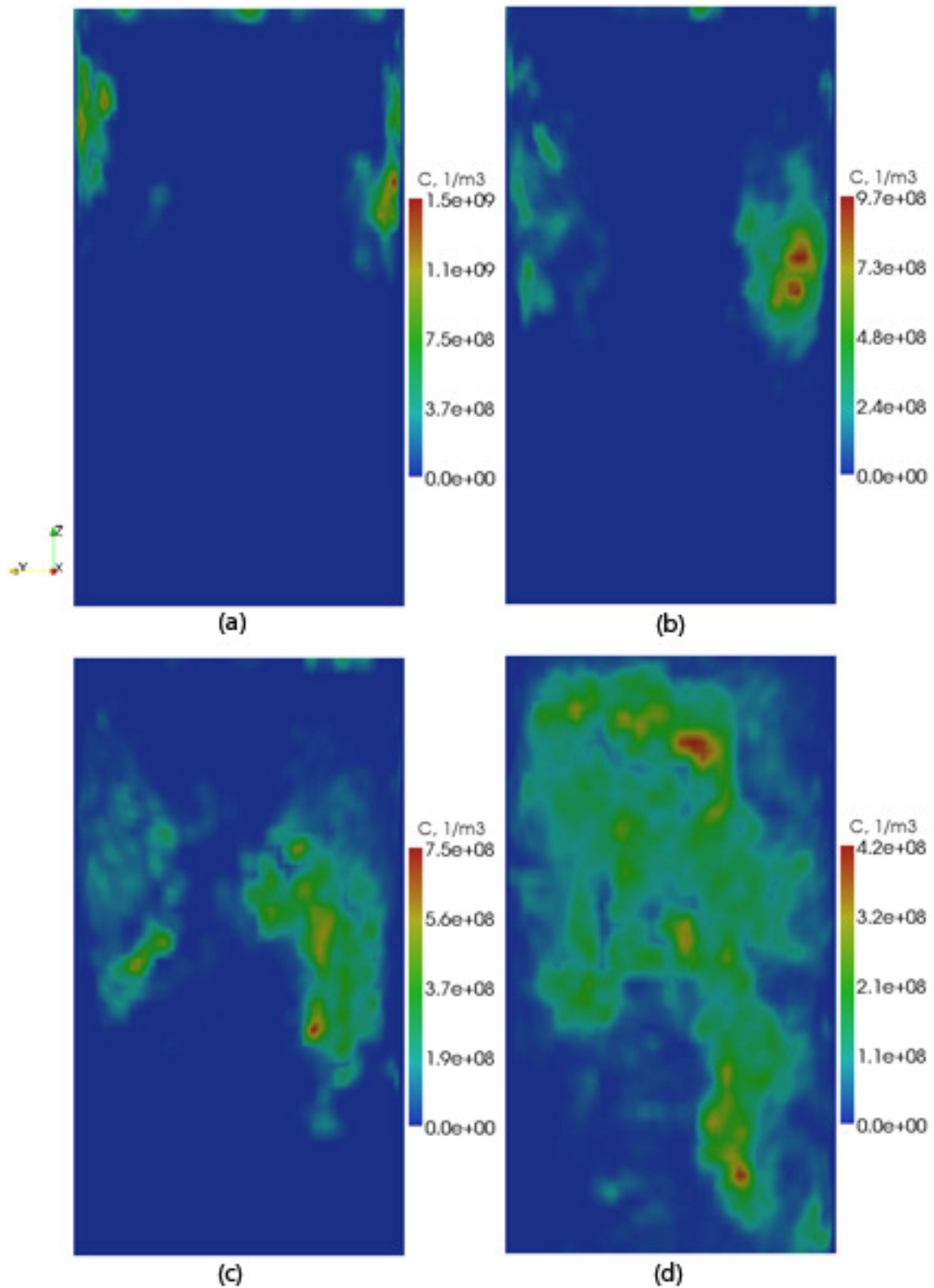


Figure 10: The evolution of the concentration of the particles with diameter 0.05 mm in ICF. Concentrations are shown in the central vertical plane. (a) – 2 s; (b) – 3 s; (c) – 4 s; (d) – 6 s.

Figure 10 shows the evolution of the small particle distribution in the central vertical plane. It is important to note that bigger particles are concentrated in the middle zone of the crucible near the wall. The rate of the concentration in this zone increases with increasing the diameter of the particles.

4 CONCLUSIONS

- Theoretical analysis of the particle motion in the EM governed turbulent flow is carried out and the model of particle transport in such flow is proposed.
- The influence of the different forces on the motion of the particles in ICF is analyzed.
- The cases with different particle relative density are simulated using two models of the behavior of the particle close to the wall: 1) the particle can not slip by the wall (approximately simulate the case of the rough wall); 2) the particle can slip by the wall (smooth wall). The results of second model qualitatively agree with the experimental results [14], thus this model should be used simulation under such conditions.
- The typically scheme of the motion of the particle cloud is obtained. The regions of the concentration of big particles are estimated.

REFERENCES

- [1] E. Dötsch, Inductive melting and holding, *Vulkan-Verlag* (2009)
- [2] K. Takatani, Effect of electromagnetic field on fluid flow, heat transfer and inclusion behavior in continuous casting process, *Magnetohydrodynamics* **32**(2), pp. 128-133 (1996)
- [3] M. Kirpo, A. Jakovics, E. Baake and B. Nacke, Particle transport in recirculated EM driven liquid metal flows. In proceeding of the *International Scientific Colloquium. Modelling for electromagnetic processing*, Hannover, Germany, pp. 249 – 255 (2008)
- [4] M. Kirpo, Modeling of turbulence properties and particle transport in recirculated flows (PhD thesis), *University of Latvia, Faculty Physics and Mathematics, Department of Physics* (2009)
- [5] M. Kirpo, A. Jakovics, B. Nacke and E. Baake, Particle transport in recirculated liquid metal flows, *COMPEL The International Journal for Computation and Mathematics in Electrical and Electronic Engineering*, **27**(2), pp. 377-386 (2008)
- [6] L. E. Landau and E. M. Lifshitz, Fluid mechanics, *Pergamon* (1959)
- [7] C. E. Brennen, Fundamentals of multiphase flow, *Cambridge University Press* (2005)
- [8] A. B. Basset, A treatise on hydrodynamics with numerous examples, **Vol. II**, *Deighton, Bell and Co* (1888)
- [9] M. A. Lavrent'ev and B. V. Shabat, Metody teorii funkciy kompleksnogo peremennogo (in Russian), *Nauka* (1973)

- [10] C. T. Crowe, M. Sommerfeld and Y. Tsuji, Multiphase flows with droplets and particles, *CRC Press* (1998)
- [11] L. Schiller and Z. Naumann, Uber die grundlegenden berechnungen bei der schwerkrafttaufbereitung (in Germany), *Ver. Deut. Ing.*, **77**, pp. 318-320 (1933)
- [12] F. Odar and W. S. Hamilton, Forces on a sphere accelerating in a viscous fluid, *J. Fluid Mech.*, **18**, pp. 302-314 (1964)
- [13] D. Legendre and J. Magnaudet, The lift force on a spherical bubble in a viscous linear shear flow, *J. Fluid Mech.*, **368**, pp. 81-126 (1998)
- [14] M. Higuchi, H. Amabai, S. Shimasaki, C. Kamata, S. Teshigawara, and S. Taniguchi, Electromagnetic separation of inclusions from molten copper by alternating electromagnetic field, In proceeding of the 6th *International Conference on Electromagnetic Processing of Materials*, Dresden, Germany, pp. 86-89 (2009)